NANOTRIBOLOGICAL PROPERTIES
OF SILICON SURFACES NANOPATTERNED
BY LASER INTERFERENCE LITHOGRAPHY

Haidong He, Haifeng Yang,* **Enlan Zhao, Jingbin Hao, Jiguo Qian, Wei Tang,**
and Hua Zhu

College of Mechanical & Electrical Engineering
China University of Mining and Technology
Xu Zhou 221116, China

*Corresponding author e-mail: yhf002 @ 163.com

Abstract

The problems caused by the adhesive force and friction force become more critical when the size of M/NEMS devices shrinks to micro/nano-scale. The nanotexture-patterned surface is an effective approach to reduce friction force on micro/nano-scale. Laser interference lithography is an attractive method to fabricate micro/nanotextures, which is maskless and allows large area periodical structures to be patterned by a couple of seconds' exposure in a simple equipment system. We fabricate various nanogrooves with different pitch and space width on silicon wafers by laser interference lithography and chemical etching. We investigate the nanotribological properties of the patterned surfaces by AFM/FFM. We show that friction on the nano/micro-scale is related to the coverage rate of the nanogrooves, which decreases with increase in the space width and decrease in the pitch.

Keywords: laser interference lithography, nanofriction, AFM, surface modification.

1. Introduction

Over the last decade, micro/nano-electromechanical systems (M/NEMS) have developed rapidly due to their smaller volume, higher integration, and excellent performance [1]. As M/NEMS devices shrink to micro/nano-scale, problems caused by adhesive and friction forces become more critical [2, 3]. Traditionally, silicon is a widely used construction material for the fabrication of M/NEMS devices and, hence, most of the investigations are directed towards enhancing its tribological performance [1, 4, 5]. Many studies have shown that surface nanopatterning is an effective way to reduce adhesive and friction forces on micro/nano-scale, due to reduction of contact area [6–10]. Various methods, such as ion-beam roughening [11], focused-ion-beam milling (FIB) [12, 13], template printing [6, 10], current-induced local anodic oxidation [14], and others [15–18], are commonly used to fabricate micro/nano-structures. Laser interference lithography is an attractive fast, and maskless method to fabricate large-area periodical structures with simple equipment, which only needs a couple of minutes of exposure and development [19–22]. The principle is based on the interference of two coherent lights that form a horizontal standing wave for a grating pattern.

In this work, we fabricated various nanogrooves with different pitch and space width on silicon surfaces by laser-interference lithography and chemical etching [23]. We investigated experimentally the friction behavior of nanotexture-patterned silicon surfaces by AFM/FFM. The results showed that their friction force decreased with increase in the fractional surface coverage.

---

2. Experiment

2.1. Experimental Setup

We use laser interference lithography for fabrication of the nanogrooves. The experimental setup is shown schematically in Fig. 1. An ultraviolet laser (DSH-355-10, Photonics Industries, USA) with a working wavelength of 355 nm serves as a light source. The laser beam passes through an electronic shutter used to control sample exposure time and is then completely reflected by a mirror (M1). The reflected beam is filled, collimated, and expanded by a beam expander. The beam expander allows the high-frequency noise to be removed from the laser beam to provide a clean Gaussian profile. An optical beam splitter divides the laser beam into two coherent parts — one is reflected and the other is transmitted and guided by a mirror (M2). The attenuators ensure that both beams are at equal power when they are cast on the samples to form interference fringes.
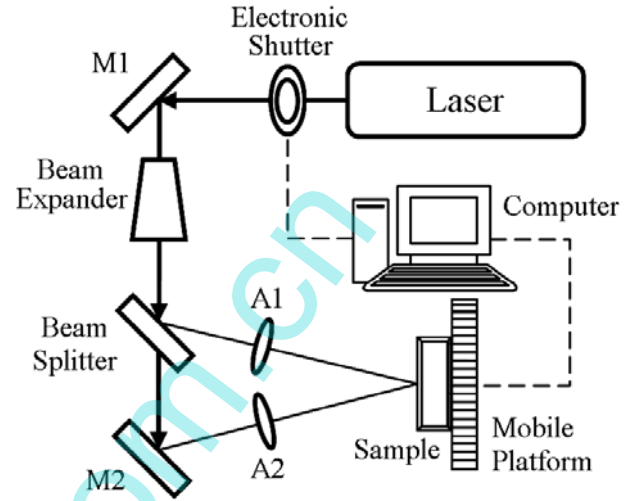

Fig. 1. Optical layout of the laser-interference lithography setup with attenuators A and mirrors M.

2.2. Fabrication Process

Experiments were carried out on N-type single-crystal silicon (100) wafers with size 1.5×1.5 cm^2. Figure 2 presents a flow chart of the fabrication process, which contains six main steps.
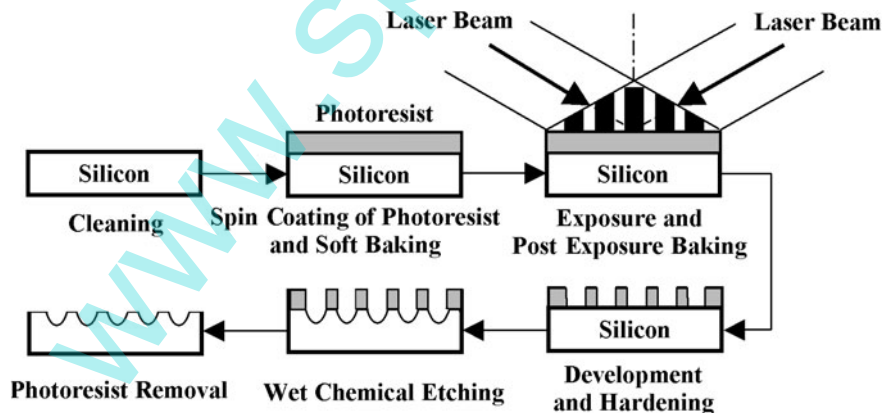

Fig. 2. Process of nanogroove fabrication by laser-interference lithography and chemical etching.

Step 1. Cleaning.
The silicon wafers were ultrasonically cleaned in acetone, absolute alcohol, and deionized water for 10 min, then baked in a drying oven at 150°C for 30 min to ensure an absolutely dry surface.

Step 2. Spin coating of photoresist and soft baking.
A positive photoresist (BP212-37) was spin coated on the polished surface of the silicon wafer using a

two-stage spinning scheme at 25°C. A spinning speed of 500 rpm and duration time of 30 s were used in the first stage, followed by the second-stage spinning with a spinning speed of 5000 rpm and duration time of 60 s. The final photoresist thickness on the wafer was about 1.25 μm. Then, the coated silicon wafers were baked in a drying oven at 90°C for 20 min to remove residual solvent from the photoresist film and improve the adhesion between photoresist and substrate, according to the photoresist manufacturer's suggestions.

Step 3. Exposure and post-exposure baking.

The laser-interference lithography setup whose optical layout is shown in Fig. 1 was used as the exposure system. The sample was fixed on the mobile platform and exposed for a few seconds (for a dose of 60–70 mJ/cm^2) to a laser of adequate power. Thus, a nanogroove pattern was recorded on the photoresist. After exposure, the silicon wafers were baked in the drying oven at 100°C for 10 min to eliminate the standing-wave effect in the photoresist film.

Step 4. Development and hardening.

The photoresist films were immersed in the positive photoresist developer (KMP PD238-II) for 15 s to remove the exposed parts and form the photoresist patterns in a water bath at 25°C, then rinsed with deionized water repeatedly. Afterwards, the samples were baked in the drying oven at 120°C for an hour, which enhances the adhesion of the photoresist on the sample surface.

Step 5. Wet chemical etching.

The wafers with patterned photoresist films, which served as etching masks, were immerged and etched with manual stirring in a mixture solution of HNO_3(65-68%):HF(40%):H_2O=2:1:1 in a water bath at 25°C for 60 s. After etching, the wafers were washed with deionized water.

Step 6. Photoresist removal.

The residual photoresist films and the reaction products in the textures were removed in the positive photoresist stripper (KMP ST600) for 30 min, and then the wafers were dried in the drying oven at 150°C after being ultrasonically cleaned by acetone and deionized water.

2.3. Nanofriction Behavior Measurement

A silicon tip sliding on a silicon surface is a suitable model system for sliding behavior in M/NEMS [10, 24]. In order to obtain the relations between surface textures and nanotribological properties, the pattern size, surface cross-section, and nanofriction behavior of the nanotexture-patterned silicon surfaces were characterized by AFM/FFM (CSPM5500 Electronics, Ben Yuan Nano-Instrument, China) using the contact mode. A silicon AFM probe with a symmetric tip shape (Budget Sensors, ContAl-G, aluminum reflex coating) and a nominal spring constant of 0.2 N/m and resonant frequency of 13 kHz was employed. Friction measurements were performed at a scanning rate of 1 Hz and scanning length of 25 μm under applied normal loads in the range of 0.1–1.8 V. All the tests were conducted at room temperature and a relative humidity of 30%.

3. Results and Discussion

3.1. Characterization of Nanogroove Si Surfaces

Laser interference lithography is a simple and easy way to change the grating period via θ adjustment by M2 and the beam splitter in Fig. 1. The interference period is calculated as $P = \lambda/(2\sin\theta)$, where
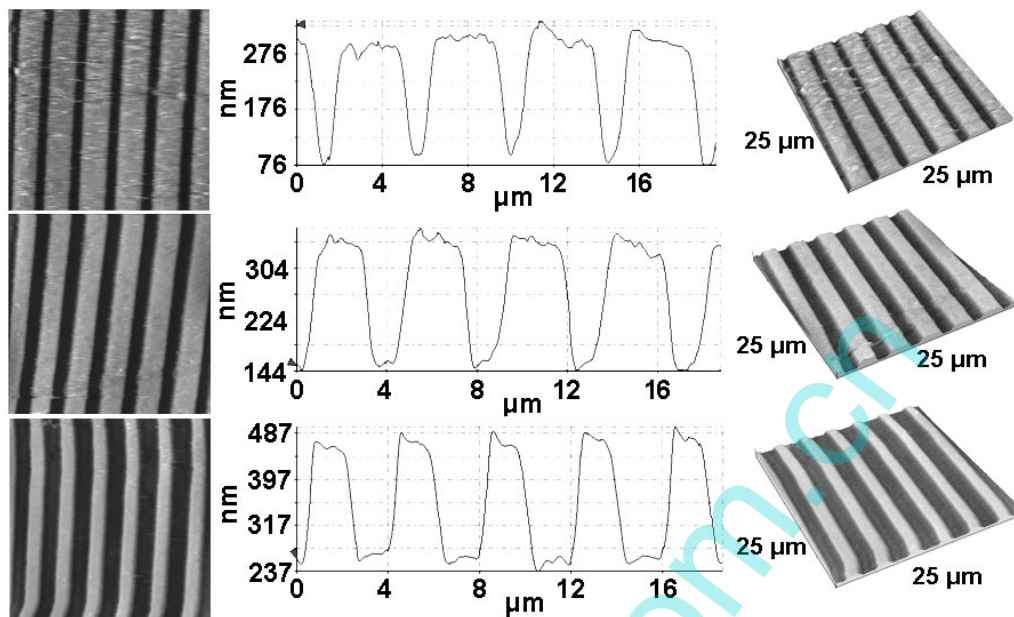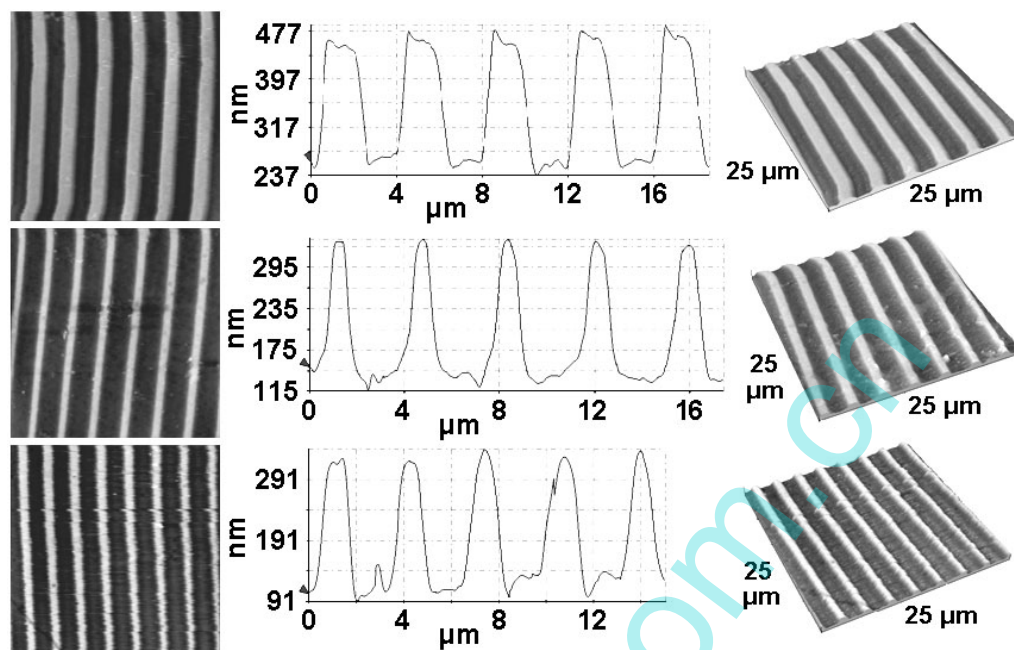
Fig. 3. 2D line section and 3D AFM images of various nanotexture-patterned silicon surfaces with different spacing width: 1.1 (top), 1.7 (middle), and 2.4 μm (bottom).

λ is the laser wavelength. The light intensity within the two-beam-interference lithography patterns is calculated as $I = 2I_0[1 + \cos(2kx\sin\theta)]$, where I_0 is determined by the laser power. Once a positive photoresist has its specific exposure dose D_p^0, it will be completely removed from the area, where the dose exceeds D_p^0. The laser dose can be controlled by the laser power and the exposure time. According to the latter formula, the laser dose is a sinusoidally distributed quantity, the maximum of which is $2I_0$, and the minimum is zero. Thus, the dose will exceed D_p^0 if the exposure time is appropriate. The part of the exposed area exceeding D_p^0, which will be etched during the etching process, increases with increase in exposure time when the laser power is invariable. In this work, the nanogrooves with the same pitches but different spacing widths were fabricated through accurately controlling the exposure time by the electronic shutter.

2D line section and 3D AFM images of various nanotexture-patterned silicon surfaces are shown in Fig. 3. The samples shown in Fig. 3 were fabricated under the same experimental parameters, including the magnitudes of θ (about $2.3°$) and etching time (60 s), but with various exposure times of 4, 6, and 8 s, respectively. Thus, they had the same pitch of 4470 nm and an approximately equal depth of 210 nm, but with varying widths of 1.1, 1.7, and 2.4 μm. In this work, we also fabricated patterned silicon surfaces with different pitches of 3.8 and 3.1 μm by adjusting θ, as shown in Fig. 4. It is obvious that the nanogrooves fabricated through laser-interference lithography and chemical etching are regular and their cliffs are smooth.

3.2. Nanofriction Properties

To investigate the nanotribological properties of silicon surfaces with different nanogrooves, we measured the nanotribological "force versus normal load" curves by AFM/FFM. The normal load and friction force were measured as a voltage signal. Each friction test was repeated 10 times. The results are pre-

Fig. 4. 2D line section and 3D AFM images of various nanotexture-patterned silicon surfaces with different pitches of 4.5 (top), 3.8 (middle), and 3.1 μm (bottom).

sented in Table 1. Figure 5 shows the average "friction force versus load" curves for the samples listed in Table 1. As seen from Fig. 5 a, the nanogrooves have equal pitch of 4.5 μm, but the friction force decreases with increase in the spacing width. In Fig. 5 b, the friction force obeys the same law as shown in Fig. 5 a, though the pitch of nanogrooves is changed from 4.5 to 3.8 μm. Figure 5 c shows the friction force of the nanogrooves with different pitches of 4.5, 3.8, and 3.1 μm. The nanopatterned surface with a pitch of 4.5 μm presented the largest friction force, and the lowest one was for a pitch of 3.1 μm.

At a nanoscale, the real area of contact and the surface strongly affect friction in the contacts for samples with the same surface chemistry, according to the fundamental law of friction given by Bowden and Tabor that $F_f = \tau A_r$, where τ is the shear strength, an interfacial property, and A_r is the real area of contact. The real area of contact depends upon the patterned fractional silicon surface coverage [8]. The nanogroove fractional surface coverage R(%) is calculated as $R(\%) = N S_{\text{space}}/S_{\text{scan}} = NW/a$, where N is the number of grooves, S_{space} and S_{scan} are the areas of the spacing and the patterned surface, respectively, W is the spacing width of the groove, and a is the length of the patterned surface perpendicular to the direction of the nanogrooves. The real contact area decreases as R (%) increases. As seen in Fig. 5 d and R (%) in Table 1, the friction force of sample 1 is the highest with a minimum coverage and sample 8 is the lowest with a

Table 1. Geometrical Parameters of Patterned Silicon Surfaces with Nanogrooves.

Sample	Pitch	Space width	Depth	R
	μm	μm	μm	%
1	4.5	1.1	0.22	24
2	4.5	2.4	0.21	53
3	4.5	1.7	0.21	39
4	4.5	1.2	0.22	27
5	4.5	1.0	0.21	23
6	3.8	1.4	0.22	37
7	3.8	2.4	0.20	64
8	3.8	2.8	0.21	74
9	3.1	2.2	0.22	71
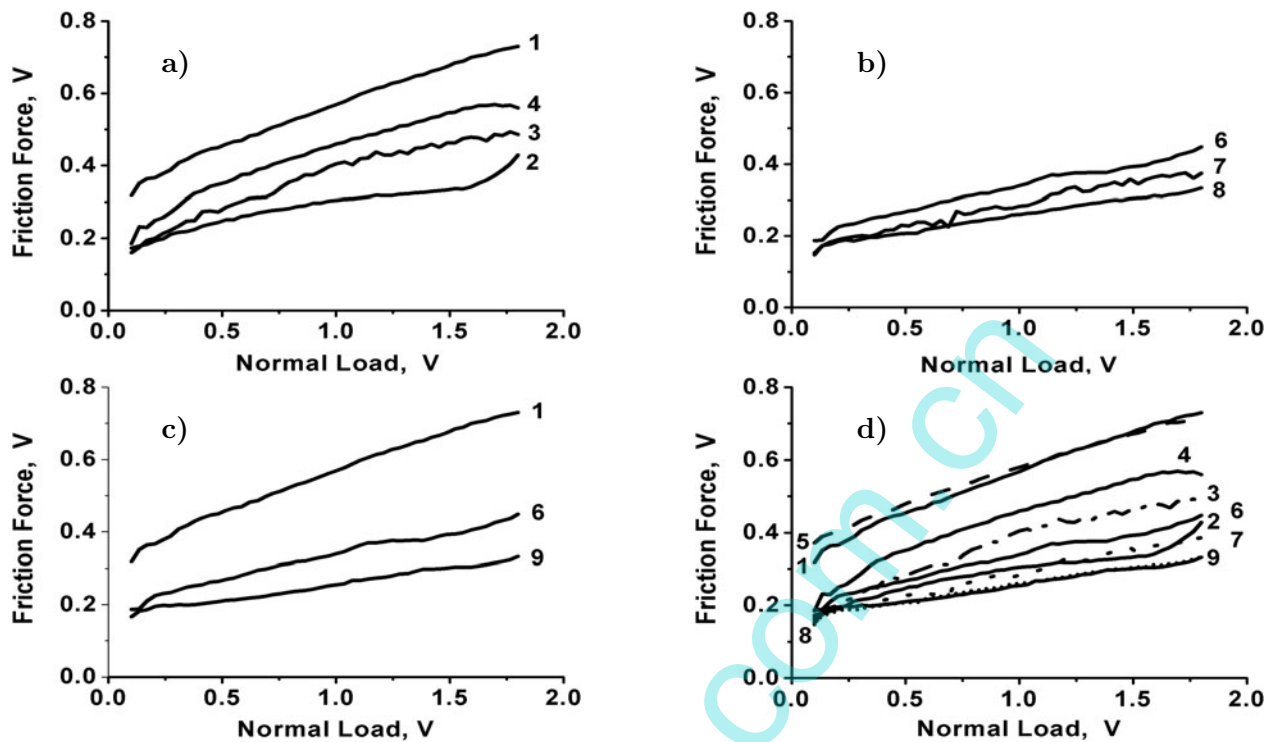
Fig. 5. Friction force versus load curves for the surfaces of the patterned silicon wafers with different fractional surface coverage. Pitch of the tested samples: 4.5 (a), 3.8 (b), 4.7 (c), and 3.8 and 3.1 μm (d). The curves are numbered in accordance with Table 1.

maximum coverage. All the tested samples obey the law that the number of asperities in the contact decreases and leads to a lower friction force with increased fractional surface coverage, though they have various geometrical dimensions of the nanogrooves.

4. Conclusions

In conclusion, various surface nanogrooves with different pitches and spacing widths were fabricated on silicon wafers using laser-interference lithography and chemical etching, and their nanotribological properties were investigated by AFM/FFM. We draw the conclusion from this work:

Laser interference lithography is an attractive approach to fabricate micro/nano-textures. It can easily change the geometrical parameters of nanogrooves.

The height of nanogrooves can be controlled by the chemical etching time.

The number of asperities in the contact decreases and leads to a lower friction force with increased fractional surface coverage.

Acknowledgments

References

1. S. M. Spearing, *Acta Mater*, **48**, 179 (2000).
2. R. A. Singh, E. S. Yoon, *Wear*, **263**, 912 (2007).
3. M. Zou, L. Cai, H. Wang, et al., *Tribol. Lett.*, **20**, 43 (2005).
4. B. Bhushan and H. Liu, *Wear*, **225-229**, 465 (1999).
5. E. S. Yoon, R. A. Singh, H. Kong, et al., *Tribol. Lett.*, **21**, 31 (2006).
6. X. Zhang, X. Wang, W. Kong, et al., *Appl. Surf. Sci.*, **258**, 113 (2011).
7. X. Zhang, Y. Lu, E. Liu, et al., *Colloids Surf. A: Physicochem. Eng. Aspects*, **401**, 90 (2012).
8. Y. Wang, L. Wang, Q. Xue, et al., *Colloids Surf. A: Physicochem. Eng. Aspects*, **372**, 139 (2010).
9. R. Arvind Singh and Eui-Sung Yoon, *Wear*, **263**, 912 (2007).
10. W. Zhao, Liping, Q. Xue, *Colloids Surf. A: Physicochem. Eng. Aspects*, **366**, 191 (2010).
11. E. S. Yoon, S. H. Yang, H. Kong, and K. H. Kim, *Tribol. Lett.*, **15**, 145 (2003).
12. Y. Ando, T. Tanaka, J. Ino, and K. Kakuta, *JSME Int. J. Ser. C*, **44**, 453 (2001).
13. Y. Ando, *Wear*, **238**, 12 (2000).
14. Y. Mo, W. Zhao, D. Huang, et al., *Ultramicroscopy*, **109**, 247 (2009).
15. J. M. Yao, X. Yan, G. Lu, et al., *Adv. Mater.*, **16**, 81 (2004).
16. N. J. Suematsu, Y. Ogawa, Y. Yamamoto, and T. Yamaguchi, *J. Colloid Interface Sci.*, **310**, 648 (2007).
17. H. Yang, L. Zhou, H. He, et al., *J. Russ. Laser Res.*, **33**, 349 (2012).
18. H. Yang, H. He, L. Zhou, et al., *Opt. Appl.*, **42**, 795 (2012).
19. Q. Xie, M. H. Hong, H. L. Tan, et al., *J. Alloys Compd.*, **449**, 261 (2008).
20. Y.-L. Yang, C.-C. Hsu, T.-L. Chang, et al., *Appl. Surf. Sci.*, **256**, 3683 (2010).
21. A. Rodriguez, M. Echeverria, M. Ellman, et al., *Microelectron. Eng.*, **86**, 973 (2009).
22. C. H. Liu, M. H. Hong, M. C. Lum, et al., *Appl. Phys. A*, **101**, 237 (2010).
23. J. Zhang and Y. Meng, *J. Mater. Process. Technol.*, **212**, 2133 (2012).
24. D. Marchetto, A. Rota, L. Calabri, et al., *Wear*, **265**, 577 (2008).